






Open Archive Toulouse Archive Ouverte (OATAO)

OATAO is an open access repository that collects the work of Toulouse researchers and makes it freely available over the web where possible.

This is an author-deposited version published in: <http://oatao.univ-toulouse.fr/>
Eprints ID: 24563

To link to this article : DOI:10.1109/EIC.2018.8481037

URL : <https://doi.org/10.1109/EIC.2018.8481037>

To cite this version: Collin, Philippe  and Malec, David  and Lefèvre, Yvan  *Tool to design the primary electrical insulation system of low voltage rotating machines fed by inverters.* (2018) In: 2018 IEEE Electrical Insulation Conference (EIC), 17 June 2018 - 20 June 2018 (San Antonio, United States)

Any correspondence concerning this service should be sent to the repository administrator:

staff-oatao@listes-diff.inp-toulouse.fr

Tool to design the primary electrical insulation system of low voltage rotating machines fed by inverters

COLLIN Philippe
LAPLACE, Université de Toulouse,
CNRS, INPT,UPS, France
collin@laplace.univ-tlse.fr

MALEC David
LAPLACE, Université de Toulouse,
CNRS, INPT,UPS, France
malec@laplace.univ-tlse.fr

LEFEVRE Yvan
LAPLACE, Université de Toulouse,
CNRS, INPT,UPS, France
lefevre@laplace.univ-tlse.fr

Abstract—In this communication, we describe a methodologic tool (software) that give instruction to design the coil winding of low voltage machines fed by inverters. The aim of this tool is to bring useful information to the coil manufacturer who has, first, to respect the size of the slots, the total copper section (slot occupancy) and the coil voltage that are imposed by the motor designer. Then, to increase the PDIV between turns and between turns and ground to the highest value. For that purpose, by using a numerical simulation that takes into account the Paschen's law, the developed software will provide how to choose and arrange the enameled wires in the slots: random or form-wound coils, wires shape (round or rectangular), number of wires in parallel by turn, insulation thickness (grade), turns arrangement,... up to find the best solution that allow to respect both motor designer and PDIV constraints. Some practical examples will be given to prove the efficiency of such a tool.

Keywords—partial discharges, electric motor, numerical simulation, design tool

I. INTRODUCTION

Until now PD phenomena were not really taken into account in the early design process of an electric machine. The manufacturer used to rely on his experience in order to build the electric insulation system.

Since the introduction of the power electronic power supplies, that provides easy control of the machine rotational speed, the electrical insulation of such motors faces new hazards. Fast changing supply voltage, with high dV/dt , may cause the apparition of partial discharges (PD), that results in accelerated insulation aging and often leads to premature failure of the motors. In low voltage rotating machines, the stator insulation system is multi-level. Its first component (primary insulation) is the polymer enamel on the magnet wire, among the others (inter-phase insulation, slot insulation and impregnation varnish). Depending on the desired thermal properties, there are several types of polymers being used nowadays in enameled wires: polyamide (PA), polyamide-

imide (PAI), polyester-imide (PEI) and polyimide (PI). Inorganic nano-particles (SiO_2 , Al_2O_3 , ZnO ,...) may be used as fillers to obtained corona-resistant enamels. In random-wound stators powered by power inverters, in comparison with sinusoidal power supply, the magnet wire insulation is far more endangered. Hence, the objective is to concentrate on this primary insulation. Once the voltage exceeds the partial discharge inception voltage (PDIV), the electric charges will start to bombard the surface of the insulator, to increase its temperature and to provoke chemical reactions. All these actions will strongly increase the insulator degradation rate. Usually, there are three ways used to avoid and/or to resist to such damage. First, the use of corona-resistant enameled wires, especially formulated to increase the lifetime under PD attacks. Second, a good design of the primary electrical insulation: choice of right enamel wires (size and shape), insulation thickness (grade), choice of wires arrangement in the slots... Third, the use of both of these two first solutions.

New challenges make necessary the PD phenomena to be taken into account by the designer especially in the aeronautical domain with the “more electric aircraft” concept. Europe is continuing a project aiming to carry the aeronautic industry toward hybrid and then full electric aircraft (Clean Sky 2). This will be done by increasing the specific power of the electric motors to 5 kW/kg in 2025 and 10 kW/kg in 2035[1]. At this level the voltage on DC bus will probably be higher than 1 kV. This will lead to an increase of the electric stress on the winding of the motors fed by inverters (Fig 1).

In order to minimize this stress a tool is under construction in order to provide to the designer the best winding configuration. This paper focuses on the design of the primary electrical insulation system of low voltage rotating machines fed by inverters. Under these conditions the voltage on the DC bus is fixed to the upper limit $V_{DC}=690V$ [2]. First, the model of the slot considered will be given. Then, the methodology to detect PD will be presented. Finally, some results from numerical

simulations performed with Ansys Mechanical APDL will justify the use of such a tool.

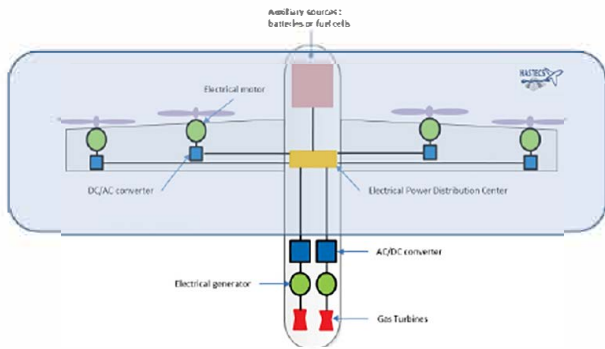


Fig 1. Electromechanical chain of full electric aircraft

II. SLOT MODELLING

The model of the slot is a first level one. One considers a slot whose sizes are $h_{slot, tot} = 1.4$ cm by $L_{slot} = 5$ mm. The slot is supposed to carry two phases. In this work only one phase is studied. The slot is then divided in two and only the lower half is drawn on Ansys Mechanical APDL as can be seen in Fig 2. The choice is made to consider 8 conductors per slot and per phase. The different nominal diameters are chosen so that the filling factor is close to 0.2 in order to have lot of free space in the slot. In all the numerical simulations, the slot sizing and the copper cross section remain constant.

There are two kinds of interface: conductor/conductor and conductor/slot. These interfaces are presented in Fig 3.

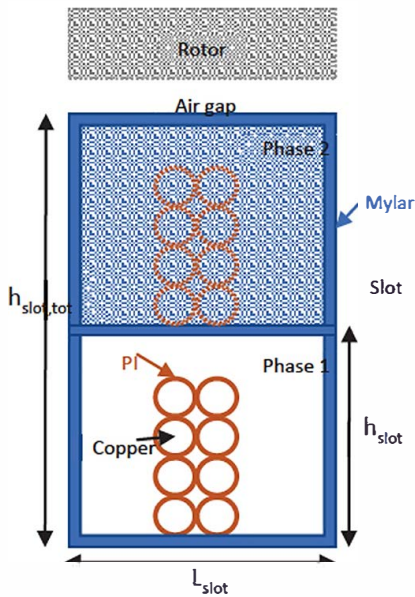


Fig 2. Slot cross section

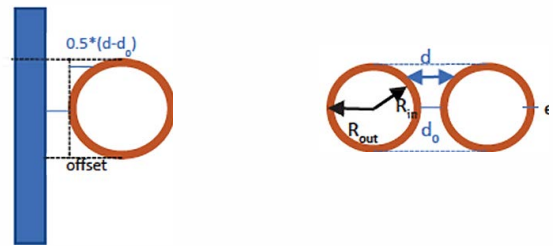


Fig 3. Interfaces (left: conductor/slot, right: conductor/conductor)

III. FIRST LOOK ON THE TOOL

The tool is coupling Matlab 2016 with Ansys Mechanical APDL. Fig 5 presents the different steps in order to determine if PD may exist. First of all, the parameters are typed in a Matlab script. This script then executes the Ansys Mechanical APDL model which proceeds to an electrostatic solution. The problem is solved in term of scalar electric potential V . Let's remind that under the following hypothesis of a linear analysis this potential V and the electric field E are linked by (1) [4]:

$$E = -\text{grad}(V) \quad (1)$$

For each interface, the potential drops over the distances d is computed on Matlab. The $V_{simu}(d)$ curves obtained are then compared to the Paschen's curve with p the pressure equals to 1 bar. If $V_{simu}(d_i) \geq V_{Paschen}(d_i)$ there are probably PD at the distance d_i .

This Paschen's curve is the experimental one measured in the air by Dakin [5]. The measurement was performed between 2 plate metallic electrodes. This experimental curve is different from the theoretical one usually found in the literature. The latest considers a uniform electric field E between the electrodes and consists in reflecting the Townsend breakdown mechanism in gases; the ionization process is carried by "primary electron" and "secondary electron" emission at the cathode by ion bombardment [6]. The experimental curve however takes into account other phenomenas such as photoionization, the ionization by light. It explains why the minimums are not the same on both curves.

As it was previously indicated, this experimental curve is obtained using 2 plate metallic electrodes. However, in the model presented here the conductors are covered with a polyimide (PI) layer. This changes the ionization mechanism especially the value of the secondary electron emission at the cathode. This coefficient is usually designed with γ in the literature. It is the ratio of the number of electrons leaving the cathode over the number of incoming ions (at the cathode). It is easy to calculate analytically γ with metallic electrodes but with electrodes covered in polymer the only way to determine it is to measure it [7] due to the complexity of the involved mechanism. Besides, in the model the interfaces are not plane/plane but rather cylindrical/cylindrical (between conductors) or cylindrical/plane (between conductor and slot).

As a first level approach the hypothesis have been done to consider a constant and straight electric field E at each interface (i.e interface plane/plane). Referring to [3], for distances $d \leq 1$ mm, the error on the electric field length is lower than 20%. For upper distances, the electric field cannot be considered as

uniform, so one cannot use Paschen's curve to determine the breakdown voltage of the air in these interfaces. In this communication, the electric field is supposed uniform (i.e. $d \leq 1\text{mm}$). Moreover, the experimental measurement of the γ coefficient between 2 round conductors covered in PI has yet to be done. In consequence, the experimental Paschen's curve given by Dakin will be used as criteria of PD existence in this work.

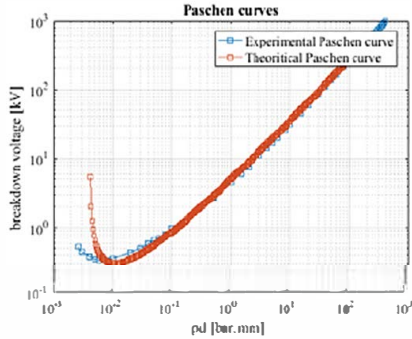


Fig 4. Paschen's curves

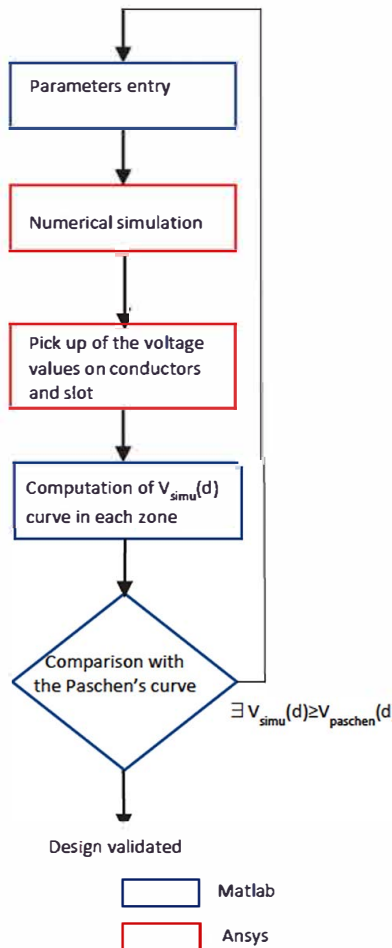


Fig 5. Overview of the process

IV. NUMERICAL SIMULATIONS

In this paragraph, 4 cases are presented which illustrates the use of this tool. As it has been introduced in part

2, the main idea is to compare the computed $V_{simu}(d)$ curves with the Paschen's curve. First the slot has been divided in zones (Fig 6). Each zone represents either a conductor/conductor or a conductor/slot interface. In all the coming curves only the zones with the highest stress (i.e. closer to the Paschen's curve) have been retained.

All the simulations have been performed under the following hypothesis:

- a star winding machine fed by an inverter working on full wave modulation.

- DC voltage bus is $U_{bus}=690\text{V}$.

- one coil per phase per slot so the voltage drop amplitude between the first and the last turn of the coil is equal to the single-phase voltage amplitude:

$$V_{coil} = \frac{U_{bus}}{2} * \sqrt{2} = 488\text{V} \quad (2)$$

However, the worst case which can happen during the transient regime is taken into account by considering an overshoot on the coil corresponding to twice the DC bus voltage. So, the voltage amplitude applied on the coil is $V_{max}=976\text{V}$. Moreover, short coil hypothesis is done so that the voltage drop between 2 consecutive turns is linear. At last it is reminded that the filling factor is chosen close to 2.

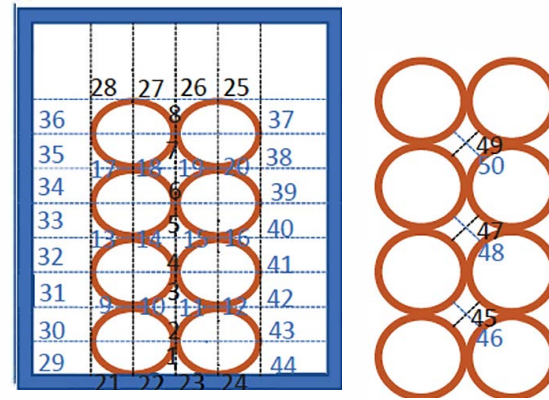


Fig 6. Zones under study

A. Turns arrangement

The first simulation consists in studying the influence of turns arrangement. For that 3 configurations have been investigated (Fig 7). The nominal diameter of the copper wires is 1.06 mm and the insulation layer is $e=17 \mu\text{m}$ [9]. Mylar thickness is fixed to $100 \mu\text{m}$ [8]. Numbers inside the copper wires refer to the turn number (i.e: 1 is the first turn and 8 is the last one). The red rectangles designated the focused zones (i.e: zones 1, 11 and 21). The 3 configurations have been chosen in the way to make the turn shift (green numbers) vary between 2 adjacent turns. Results are presented on Fig 8 and summarized on Table 1 (values taken at $d=0.01\text{mm}$). One notices that in zone 21 the voltage value at $d=0.01\text{mm}$ remains constant whatever the case. That is because the turn drop at this interface does not change. The same can be said for the voltage value of zone 1 in the better and optimal case.

Zone	V(d=0.01mm) worst case (kV)	V(d=0.01mm) better case (kV)	V(d=0.01mm) optimal case (kV)
1	0.543	0.078	0.078
10	0.337	0.253	0.168
21	0.183	0.183	0.183
Zone	$\frac{V_{\text{worst}} - V_{\text{better}}}{V_{\text{worst}}}$	$\frac{V_{\text{better}} - V_{\text{optimal}}}{V_{\text{better}}}$	$\frac{V_{\text{worst}} - V_{\text{optimal}}}{V_{\text{worst}}}$
1	86%	0%	86%
10	25%	34%	50%
21	0%	0%	0%

Table 1. Voltage values (top) and voltage reduction (low) for 3 turns arrangement

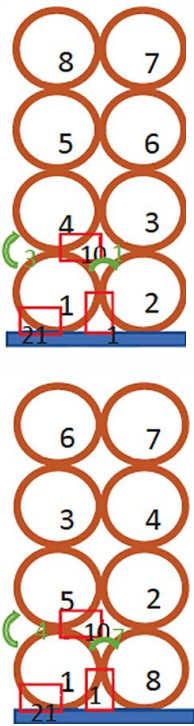


Fig 7. 3 turns arrangement: top left: worst case, top right: better case, low: optimal case

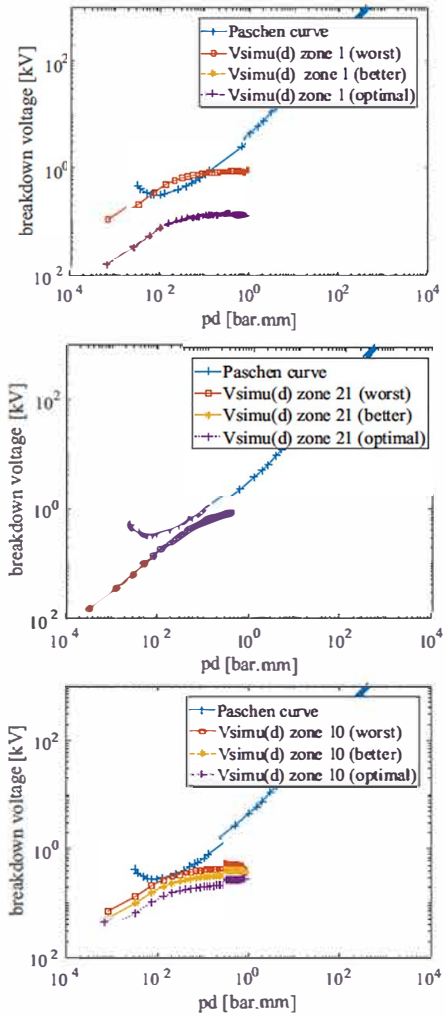


Fig 8. $V_{\text{simu}}(d)$ vs $V_{\text{Paschen}}(d)$ in zones 1 (top), 21 (middle) and 10 (low) for different turns arrangement

B. Grade influence

Here the winding is formed of 8 wires which nominal diameter is 1.12 mm. They are connected so that they form 2 turns (1 and 2) as shown in Fig 9. Mylar thickness remains fixed to 100 μm [8]. The results obtained in zone 16 are presented in Fig 10 and are summarized in the following table:

Zone	V (d=0.027 mm) min grade 3 (e=49 μm) [9]	V (d=0.027 mm) average grade 3 (e=56.5 μm)	V (d=0.027 mm) max grade 3 (e=64 μm) [9]
16	0.514 kV	0.48 kV	0.45 kV
Zone	$\frac{V_{\text{min}_{gd3}} - V_{\text{av}_{gd3}}}{V_{\text{min}_{gd3}}}$	$\frac{V_{\text{av}_{gd3}} - V_{\text{max}_{gd3}}}{V_{\text{av}_{gd3}}}$	$\frac{V_{\text{min}_{gd3}} - V_{\text{max}_{gd3}}}{V_{\text{min}_{gd3}}}$
16	6.6%	6.3%	12.5%

Table 2. Voltage values (top) and voltage reduction (low) for 3 enamel thickness

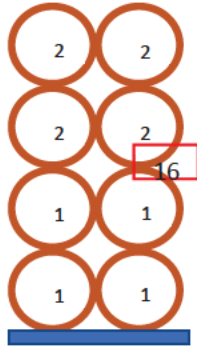


Fig 9. Configuration for grade influence simulation

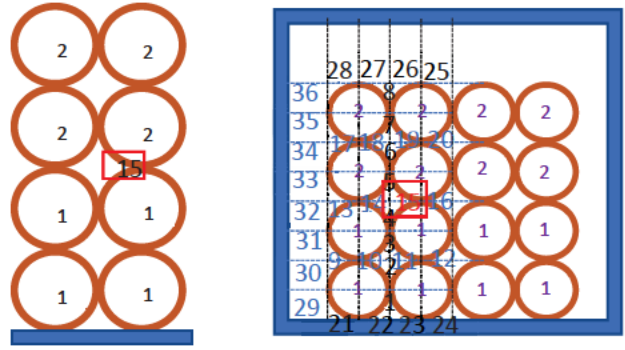


Fig 11. Left: 8 conductors, right: 16 conductors

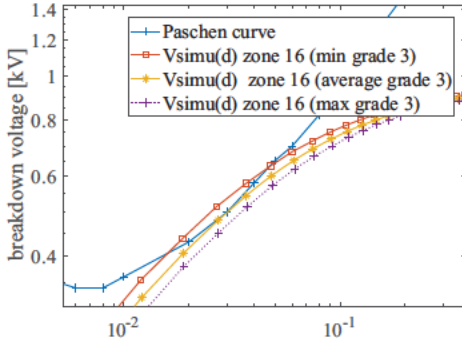


Fig 10. $V_{simu}(d)$ vs $V_{Paschen}(d)$ in zone 16 for 3 enamel thickness

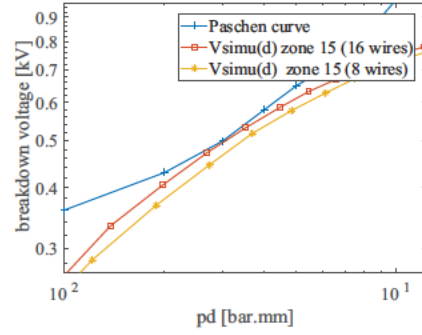


Fig 12. $V_{simu}(d)$ vs $V_{Paschen}(d)$ in zone 15 for 8 and 16 conductors

C. Number of wires

The purpose here is to study the influence of the wires diameter in PD ignition. Two cases are considered. The first one is the same than the one studied in part 3.b with $e=56.5 \mu\text{m}$ (average grade 3). The second corresponds of 16 wires of 0.8 mm nominal diameter forming 2 turns. The corresponding average enamel layer is $e=49 \mu\text{m}$. The sizing of the wires is done so that the copper cross section is equal in both case. The focus is made on zone 15 delimited by the red rectangle in Fig 11.

Zone	V (d=0.027 mm) 16 wires	V (d=0.027 mm) 8 wires
15	0.472 kV	0.446 kV
Zone	$\frac{V_{16wires} - V_{8wires}}{V_{16wires}}$	
15	5.5%	

Table 3. Voltage values (top) and voltage reduction (low) for 8 vs 16 conductors' simulation

D. Influence of d_0

The last simulation highlights the impact of the distance (d_0) between adjacent conductors. The winding configuration is similar to the one introduced in part 3.b except that the wire nominal diameter is taken to 1.06 mm and the insulation layer is $e=32 \mu\text{m}$ (max grade 1) [9]. Two cases are studied. In the first one $d_0=0$ and in the second $d_0=100 \mu\text{m}$ Fig 13. In both cases the Mylar thickness remains fixed to $100 \mu\text{m}$ [8]. The zone under focus is the zone 15. Results indicate that by increasing the distance d_0 , the $V_{simu}(d)$ curve is cut off the lowest d values. For $d_0=100 \mu\text{m}$, all the d values for which $V_{simu}(d) > V_{Paschen}(d)$ have been cut off: there is probably no more partial discharges.

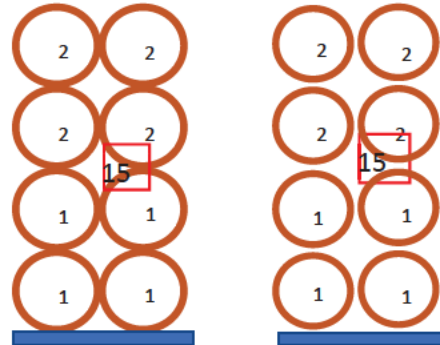


Fig 13. Configuration for d_0 influence simulation

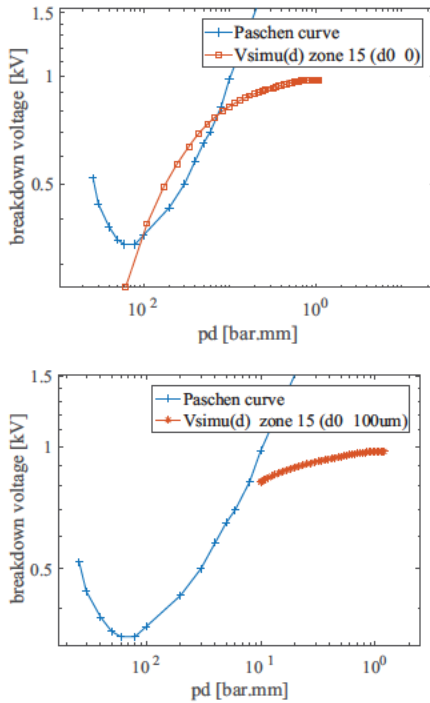


Fig 14. $V_{simu}(d)$ vs $V_{Paschen}(d)$ in zone 15 for $d_0 = 0$ (top) and $d_0 = 100 \mu m$ (low)

V. CONCLUSION

First results were presented in this paper. They illustrate the use of such a tool in the design process. Experimental validations are under progress. Then the work will be oriented in order to make this tool user friendly and fully automatized. In this paper, the geometry of the slot and the shape of the wires (circular) has been kept constant. In the future, the tool will propose a reshape of these elements if no solution can be found by playing only with the wires arrangement and the insulation thickness. This tool is clearly in interaction with both the magnetic and thermal sizing of the machine design.

ACKNOWLEDGMENT

This project has received funding from the Clean Sky 2 Joint Undertaking under the European Union's Horizon 2020 research and innovation program under grant agreement No 715483.

REFERENCES

- [1] Hybrid Aircraft Academic reSearch on Thermal & Electrical Components and Systems (HASTECS), Project selected from CFP in Cleansky II (H2020) framework
- [2] Greg C.STONE, Edward A.BOULTER, Ian CULBERT, Hussein DHIRANI, "Electrical Insulation For Rotating Machines, Design, Evaluation, Aging, Testing and Repair", IEEE press series on Power Engineering, 2004
- [3] M. Loucif Benmamas, "Méthodes d'évaluation du risque de décharges partielles dans le bobinage de machines électriques destinées à la traction automobile", Phd Université PARIS SACLAY, France, 2017
- [4] "Steps in an h Method Electrostatic Analysis", ANSYS help Viewer, ANSYS MECHANICAL APDL
- [5] T.W. Dakin et al, "Breakdown of gases in uniform fields Paschen curves for nitrogen, air and sulfur hexafluoride", ELECTRA N 32, pp 61 81
- [6] F. Koliatene, Th. Lebey, J.P Cambronne, S. Dinculescu, "Impact of the aeronautic environment on the Partial Discharges Ignition: A basic study", Conference Record of the 2008 IEEE International Symposium on Electric Insulation, ISEI, 2008
- [7] A. Shih, J. Yater, C. Hor, and R. Abrams, "Secondary electron emission studies", *Applied surface science*, vol. 111, pp. 251 258, 1997
- [8] SYNPLEX, Mylar® A, Synflex Elektro GmbH
- [9] SONA™, Enamelled Copper Wire